Potentials of Polyacrylonitrile Substitution by Lignin for Continuous Manufactured Lignin/Polyacrylonitrile-Blend-Based Carbon Fibers

Daniel Sebastian Jens Wolz [1,2], Robert Seidel-Greiff [1,2,*], Thomas Behnisch [1,2], Iris Kruppke [2,3], Irina Kuznik [2,3], Paul Bertram [2,3], Hubert Jäger [1,2], Maik Gude [1,2] and Chokri Cherif [2,3]

1 Institute of Lightweight Engineering and Polymer Technology, Technische Universität Dresden, Holbeinstraße 3, 01307 Dresden, Germany; daniel_sebastian.wolz@tu-dresden.de (D.S.J.W.); thomas.behnisch@tu-dresden.de (T.B.); hubert.jaeger@tu-dresden.de (H.J.); maik.gude@tu-dresden.de (M.G.)

2 Research Center Carbon Fibers Saxony (RCCF), Technische Universität Dresden, Breitscheidstr. 78, 01237 Dresden, Germany; iris.kruppke@tu-dresden.de (I.K.); irina.kuznik@tu-dresden.de (I.K.); paul.bertram1@tu-dresden.de (P.B.); chokri.cherif@tu-dresden.de (C.C.)

3 Institute of Textile Machinery and High Performance Material Technology, Technische Universität Dresden, Hohe Straße 6, 01069 Dresden, Germany

* Correspondence: robert.seidel-greiff@tu-dresden.de; Tel.: +49-351-463-42891

Abstract: While carbon fibers (CFs) are still the most attractive reinforcement material for lightweight structures, they are mostly manufactured using crude oil-based process chains. To achieve a higher eco-efficiency, the partial substitution of polyacrylonitrile (PAN) by renewable materials, such as lignin, is investigated. So far, this investigation has only been carried out for batch manufacturing studies, neglecting the transfer and validation to continuous CF manufacturing. Therefore, this work is the first to investigate the possibility of partial substituting lignin for PAN in a continuous process. Lignin/PAN-blended CFs with up to 15 wt.-% lignin were able to attain mechanical properties comparable to unmodified PAN-based carbon fibers, achieving tensile strengths of up to 2466 MPa and a Young's Modulus of 200 Pa. In summary, this study provides the basis for continuous Lignin/PAN-blended CF manufacturing.

Keywords: lignin; polyacrylonitrile; blend; carbon fibers; tensile properties; continuous processes

1. Introduction

Renowned for their exceptional mechanical and electrical properties, carbon fibers (CFs) have long been integral to lightweight construction applications within the aerospace [1,2], civil engineering [3], and energy storage [4] industry. Since the 1950s, the production of carbon fibers has relied on a consistent manufacturing process. This process involves creating a precursor fiber (PF) from a polymer material, usually derived from petroleum, primarily polyacrylonitrile (PAN). Subsequently, the PAN-based PF (PAN-PF) undergoes various thermal conversion stages, including stabilization in a thermo-oxidative environment as well as carbonization and, if desired, graphitization, both carried out in inert atmospheres [2,3].

Especially in times of climate change, a resource-efficient and climate-friendly industry is needed to slow down the greenhouse effect. For CFs, the aim is to replace PAN with renewable carbon-rich additives, such as lignin and/or cellulose. Up to 30% of the dry mass of lignifying plants consists of lignin, which accounts for up to 70% of the CO_2 absorbed by plants [5]. For this reason, the use of fully renewable materials for CF production is being investigated [4,6,7]. Regrettably, these entirely renewable carbon fibers do not presently achieve the full spectrum of properties exhibited by PAN-based carbon fibers during the carbonization process, particularly concerning temperatures up to 1600 °C [8].

With the upcoming production of renewable PAN [9–11], there have been many attempts to partially replace PAN with renewable resources such as lignin [12–22]. In this way, the benefits of thermal processing for PAN-based carbon fibers, including their superior temperature–mechanical property relationships, can be merged with the advantages of incorporating lignin additives, which offer abundant and cost-effective raw materials. Simultaneously, the drawbacks associated with PAN-PF processing, such as the management of toxic exhaust gases [23–25], and the substantial energy requirements for graphitization in ultra-high temperature furnaces can be mitigated.

Lignin/PAN-blend CFs have been produced batch-wise with lignin contents up to 25 wt.-% with mechanical properties up to 148 GPa tensile modulus and 1.3 GPa tensile strength [17]. This could be further increased by the addition of carbon nano tubes (CNTs) for CNT/Lignin/PAN-blend CFs with lignin contents up to 30 wt.-% for a tensile modulus of 200 GPa and a tensile strength of 1.4 GPa [21]. Still, lignin additives lead, in many studies, to pore and defect initiation during thermal conversion due to the inhomogeneous structure of lignin and therefore to CFs with more defects [4,20,26]. The influence of various factors additionally to lignin content [12,17,20,21] has been studied, including lignin distribution [13,14], the molar mass of the lignin [15,18], the use of Lignin-PAN-co-polymers [16,19,22] and the functionalization of lignin for enhanced Lignin/PAN-blend CFs.

As most studies are performed in batch processing [12–22], only a few investigations focus on the influence of lignin content on continuous processing [27]. In continuous thermal conversion, various factors interact, necessitating the need to distinguish and isolate their individual influences. So far, there have been no mechanical properties published for continuously produced Lignin/PAN-blend-based CFs. Therefore, the aim of this study is to investigate the influence of increasing lignin contents on the mechanical properties of Lignin/PAN-blend-based CFs in continuous thermal conversion.

2. Materials and Methods

2.1. Materials

Lignosulfonate (LS) with a low sulfonate content (<4%) and a molecular weight of approx. 10,000 g/mol, as well as dimethyl sulfoxide (DMSO, 99%), were purchased from *Sigma-Aldrich, Merck KGaA, Darmstadt, Germany*. Dimethylformamide (DMF, 99%) was purchased from *BCD Chemie GmbH Hamburg, Hamburg, Germany*. Pyridine (>99%) and acetic anhydride (>99%) were purchased from *VWR International GmbH, Radnor, PA, USA*. An institute's own PAN polymer with a number average molar mass of 119,000 ± 3100 g/mol and a polydispersity of 2.7 ± 0.1 was purchased, which was previously used in [28–30].

To maintain the economic characteristics of lignin with minimal preprocessing [20] and enhance its solubility, both raw and minimally modified, esterified lignin have been employed as raw materials. For lignin esterification, 100.0 g of LS was dried at 60 °C in a drying cabinet and then dissolved in 500.0 g of DMSO while stirring vigorously. Then, 184.2 g (1.80 mmol) of acetic anhydride and 142.7 g (1.80 mmol) of pyridine were added successively and the reaction solution was stirred for 20 h under air atmosphere. The lignin was then precipitated in approx. 3 L of distilled water, centrifuged, again suspended in approx. 1 L, and finally centrifuged. The esterified lignin (AcL) was dried in a drying cabinet at 60 °C and finally crushed with a mortar.

2.2. Precursor Fiber Spinning

The reference spinning solution was prepared from 18 wt.-% PAN and 82 wt.-% DMF-based solvent. LS/PAN-blend solutions were provided analogous to the reference, and 1 wt.-%, 2 wt.-%, 5 wt.-%, 10 wt.-%, 15 wt.-% and 20 wt.-% LS (related to PAN) were added gradually. Although the LS contents were examined up to 20 wt.-%, it was only feasible to create homogeneous AcL solutions up to a concentration of 10 wt.-%. Accordingly, AcL/PAN-blend solutions were prepared mirroring the reference and augmented with

1 wt.-%, 2 wt.-%, 5 wt.-%, and 10 wt.-% AcL. These solutions were homogenized by stirring at 60 °C and then degassed under vacuum.

The fiber spinning was carried out in a wet-spinning pilot plant consisting of one coagulation bath, three washing baths, one drying unit, one sizing unit, and a winder [31]. The spinning solutions were heated to 70 °C and extruded through a filter (50 μm) and a spinneret with 1008 holes and spin nozzles with a diameter of 70 μm. The spinneret was immersed in the coagulation bath, and fiber was converted with a jet stretch of 1.0 (without stretching). The fibers were subsequently drawn within the washing baths to an overall ratio of 1:4.0, dried, and finally sized with Torsinol ZSB spin finish. The spinning of the fiber was successful for all the fibers mentioned in the paper. More in-depth details are the subject of unpublished studies.

2.3. Thermal Conversion

The thermal conversion proceeded in continuous process lines, consisting of a stabilization line and a carbonization line. The continuous thermo-oxidative stabilization line [32] consists of an oven with four heating zones (HZi) and as many processing units. The temperature profile was set to 245 °C to 255 °C for HZ1 ($T_{STAB,HZ1}$), 260 °C to 270 °C for HZ2 ($T_{STAB,HZ2}$), 280 °C to 285 °C for HZ3 ($T_{STAB,HZ3}$), and 290 °C to 300 °C for HZ4 ($T_{STAB,HZ4}$). The minor temperature variations within one HZ are related to an investigation into the influence of different temperature gradients as lignin can exhibit sensitive behavior at higher temperatures [33]. However, the gradients were so small that they had no influence on the process results and are therefore negligible in this study.
The cumulative residence time in stabilization (t_{STAB}) was adapted to 120 min based on the experience of previous trials. The fiber stretch was set to $\epsilon_{pre} = 0.49\%$; $\epsilon_{HZ1} = 0.48\%$; $\epsilon_{HZ2} = 0.51\%$; $\epsilon_{HZ3} = 0.29\%$; $\epsilon_{HZ4} = 0.32\%$; and $\epsilon_{post} = 1.6\%$.

The carbonization line consists of a low temperature (LT) and a high temperature (HT) furnace in series, each with four separate heating zones. The temperature profile is set for LT to 450 °C, 550 °C, 650 °C, and 800 °C and for the HT to 900 °C, 1050 °C, 1200 °C, and 1400 °C. The fiber stretch was set to −7.6% with a dwell time of 8 min. An overview of the parameter setups can be seen in Table 1. The nomenclature of the labels was carried out by combining the abbreviation of lignin functionalization (LS, AcL) and the lignin content. The groups of samples with either LS or AcL additive are further referred to as *LSi* and *AcLi*, where i is the additive content.

Table 1. Varied process parameters for lignin content (x_{Lig}) and lignin functionalization (Lig), dwell time in stabilization (t_{STAB}), temperature of the heating zones 1 to 4 in stabilization ($T_{STAB,HZi}$), and maximum temperature in carbonization ($T_{CARB,max}$).

Label	x_{Lig}	Lig	t_{STAB}	$T_{STAB,HZ1}$	$T_{STAB,HZ2}$	$T_{STAB,HZ3}$	$T_{STAB,HZ4}$	$T_{CARB,max}$
PAN	-		120	250	280	285	295	1400
LS1	1	LS	120	255	280	280	295	1400
LS2	2	LS	120	245	280	290	295	1400
LS5	5	LS	120	255	270	290	295	1400
LS10	10	LS	120	255	260	285	300	1400
LS15	15	LS	120	250	270	280	290	1400
LS20	20	LS	120	250	260	290	295	1400
AcL1	1	AcL	120	255	280	280	295	1400
AcL2	2	AcL	120	245	280	290	295	1400
AcL5	5	AcL	120	245	280	285	295	1400
AcL10a	10	AcL	120	255	270	285	295	1400
AcL10b	10	AcL	120	250	260	285	300	1400

2.4. Characterization

Single filament tensile tests were carried out with a Textechno Favimat+ with a 210 cN measuring head at 20 mm gauge length. The fineness was measured by vibroscope method.

The pretension was 0.5 cN/tex, and the test speed 2 mm/min. Thirty filament samples were taken for each CF measurement. The density was measured by means of a floating method according to DIN 65569 [34].

Filament diameters were determined by the production of micrographs using a Carl Zeiss Axio 100 light microscope. At a resolution of 1:100, sections with more than 50 filaments were selected and the filament diameter was measured with Olympus Stream Essentials at 400× magnification.

Thermogravimetrical analyses (TGA) were carried out with a STA 409 PC/PG from NETZSCH. Approx. 24 mg of each sample was investigated in alumina oxide crucibles. The samples were heated from 30 °C with 2 K/min to a temperature of 400 °C. A synthetic air atmosphere with 75 ml/min was applied.

Differential scanning calorimetry (DSC) measurements were conducted with a DSC Star 1 from Texas Instruments. Approx. 3 mg of each sample was examined under air atmosphere with a flow rate of 40 ml/min and a heating ramp of 5 K/min from 150 °C to 400 °C. The evaluation of reaction enthalpy was performed by integrating the areas between 230 °C and 380 °C with a spline baseline. Afterwards, the stabilization index SI was calculated for the residual enthalpy of the stabilized fiber (h_{SF}) in regard to the precursor fiber (h_{PF}) [35].

$$SI[\%] = 100 * (1 - h_{SF}/h_{PF}) \tag{1}$$

3. Results and Discussion

Influence of Lignin Contents

All precursor fibers except *LS*5 and *LS*20 could be thermally converted. The thermal stabilization of *LS*5 and *LS*20 was not possible because of their PF brittleness. Cross-sectional images of a batch-processed stabilized fiber of *LS*20 show the increasing presence of macro pores in the sheath area (Figure A1). In cross-sectional images of LS/PAN-blend CFs, namely, *LS*1, *LS*2, and *LS*10, pores are discernible both within the core and in the sheath area, particularly at elevated concentrations, see Figure 1.
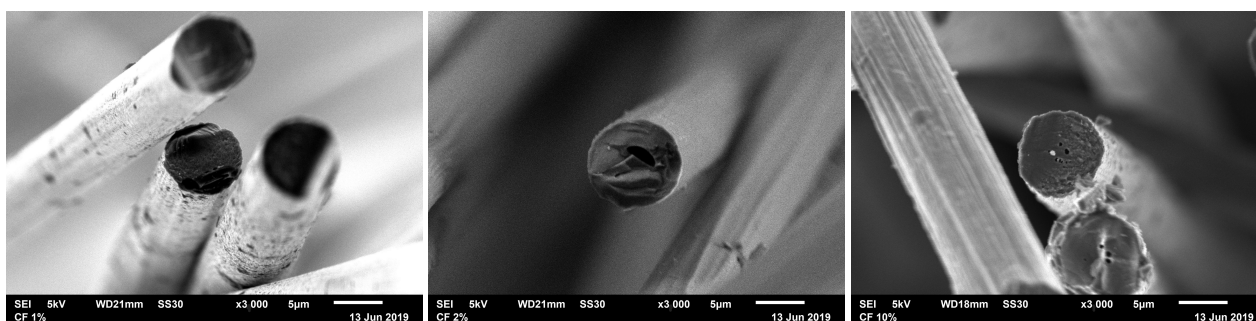

Figure 1. Cross-sectional images of CFs with different LS content: (**left**) 1 wt.-%, (**center**) 2 wt.-%, and (**right**) 10 wt.-%.

These macro pores indicate the degradation of LS and thereby the evolution of macro pores, which lead to low tensile strength and therefore fiber breakage. While *LS*20 may show too many pores for textile processing, *LS*5 seems to have agglomerated LS or random macro pores along the fiber length. As *LS*10 could be converted to CFs, the agglomeration hypothesis seems more likely, as the LS content is twice as high in *LS*10 as in *LS*5. This is further supported by the absence of a significant difference in the SI. While *PAN* has a SI of 98%, the *LSi* shows an SI between 98% for *LS*1 and 93% for *LS*15 (Figure A2). Simultaneously, the SI of *AcLi* ranges between 97% for *AcL*1 and 94% for *AcL*10. Therefore, the SI of *AcLi* fibers tends towards slightly lower values than the SI of *LSi* fibers. Finally, the difficulty of the conversion of LS/PAN-blend fibers can also be seen in thermo-gravimetric analyses as presented in Figure 2.

The thermographs for a maximum temperature of 400 °C can be interpreted as follows. The unmodified PAN fibers show the highest mass loss of 17 wt.-%. The AcL/PAN-blend

fibers with 1 wt.-% AcL content show the lowest mass loss of 13 wt.-%. The mass loss increases with higher additive AcL content up to 16 wt.-% for 10 wt.-% AcL content. Accordingly, LS/PAN-blend fibers also loose 16 wt.-% of the initial mass for 10 wt.-% LS content, whereas fibers with 15 wt.-% LS content show a weight loss of 17 wt.-%. These figures equal the behavior of the unmodified PAN-PF. The mass loss increases further for 20 wt.-%.
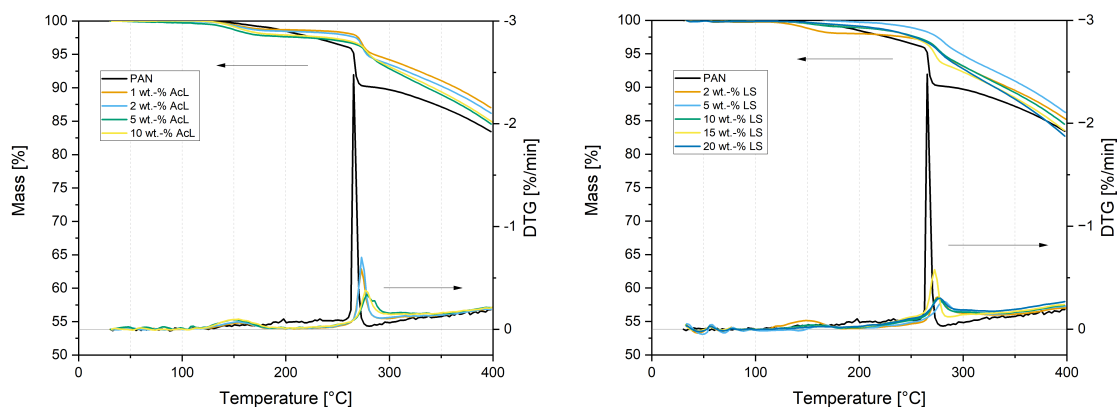
Figure 2. Thermogravimetrical analysis of the mass losses of AcL/PAN-blend-based (**left**) and LS/PAN-blend-based (**right**) precursor fibers against temperature under air atmosphere.

In the differential thermo-gravimetric (DTG) curves, a theoretically heightened presence of LS should manifest as an elevated peak in the DTG value, ideally positioned between the 15 wt.-% and unmodified DTG curves. However, this is not observed. Conversely, for the degradation rate, the 20 wt.-% LS variant aligns consistently with the remaining modification curves. A plausible explanation is that in the event of a uniform dispersion of LS particles in the 20 wt.-% variant, a distinct and elevated peak would be evident. The absence of such a peak, coupled with the congruence in degradation behavior with other loading variants, suggests indications of LS particle agglomeration. In agglomerated states, particles cluster together, leading to a slower degradation process compared to well-dispersed counterparts. Thus, achieving the homogeneous modification of PAN-blend fibers with LS contents (LS) beyond 10 wt.-% appears to pose a considerable challenge.

Moreover, all other Lignin/PAN-blend- and unmodified PAN-PF could be converted into CFs. Figure 3 illustrates the mechanical characteristics of carbon fibers with varying additive concentrations, specifically presenting data on both tensile strength and Young's modulus. The values, a detailed description of their gamma distribution parameters, and cumulative distribution graphs are given in Tables A1 and A2 and Figure A3.

A gamma distribution was chosen because it offers greater flexibility compared to a Weibull distribution fit. The data pertaining to tensile strength and Young's modulus exhibit slightly skewed characteristics and also vary across different materials. Consequently, the gamma distribution is selected to offer the most suitable fit. Its ability to accommodate skewed data and variability across materials makes it a preferred choice in this scenario.

Considering the standard deviation of the available measurements up to 10 wt.-% additive content, no significant change in tensile strength can be identified for both LS- and AcL-blended CFs. The average values vary between 1800 and nearly 2500 MPa. However, the tensile strength of 15 wt.-% LS content CFs shows a significant decrease down to 1000 MPa. Since the tensile strength of CFs indicates a decrease with a higher lignin content than 10 wt.-% (Figure 3), fiber breakage could be caused by the aforementioned pore formation induced by the lignin additives. The pore formation could further have been the result of an increased initial stabilization temperature and thus have accelerated incomplete conversion to stabilized PAN-fibers [36,37]. These increased reaction kinetics could lead to enhanced decomposition reactions, resulting in decreased tensile strengths.

Regarding the results of the Young´s modulus, a plateau between 172 GPa and 216 GPa can be identified for 0 wt.-% to 10 wt.-% additive content and for both kinds of lignin modification. Other than the tensile strength, the Young's modulus of 15 wt.-% LS content stays within the results of all the lower contents. As the filament diameter and fineness of the CFs show no significant trend with respect to the lignin modification content (Figure A4), this can be seen as a non-influence of lignin modification. In contrast to reported studies [20] indicating a decrease in fiber diameter with rising lignin concentration, our examination of LS/PAN-blend carbon fibers reveals a subtle increase in both fineness and diameter. However, it is noteworthy that this observed rise falls within the realm of standard deviation, thereby suggesting no statistically significant influence as the concentration of the additive increases (Figure A4).
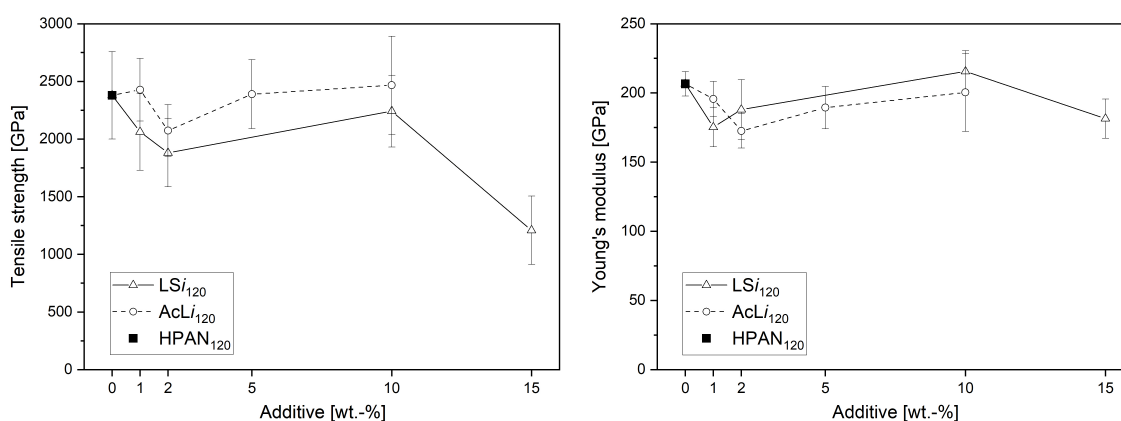
Figure 3. Behavior of tensile strength (**left**) and Young's modulus (**right**) in regard to different lignin contents for lignosulfonate (LS)/ and acetylated lignin (AcL)/PAN-blend-based carbon fibers.

The previously mentioned results might indicate a gentle rise of AcL/PAN-blend CF tensile strength with increasing additive content between 2 wt.-% and 10 wt.-%. To confirm the data, *AcL*10*a* has therefore been reproduced for a closer inspection on its mechanical properties. Despite slight changes in its temperature profile during stabilization (compare Figure 1), *AcL*10*b* achieves similar mechanical properties to those of *AcL*10*a*. The Young's modulus decreases by -8.5% to 185 GPa and the tensile strength decreases by -4.3% to 2360 MPa. However, these values can be considered equivalent because their standard deviations still overlap.

Therefore it has to be stated that an increase of up to 10 wt.-% of lignin additive has no significant impact on the mechanical properties of AcL-modified CFs. Yet, LS modification seems to have more influence. Neither of the modifications significantly alters the values of the Young's modulus.

4. Conclusions

This study has demonstrated the continuous production of Lignin/PAN-blend carbon fibers. While PAN-blend fibers could only undergo modification up to 10 wt.-% AcL content, blends with LS demonstrated the capability to be modified up to 20 wt.-%. There is still a need for the further investigation of LS/PAN-blend fibers in regard to homogeneously dispersion of LS within the precursor fibers. To the authors' knowledge, there has been no continuously produced blend CFs made from lignin and synthetic polymers published so far. Up to now, there has been only batch processed blend CFs [12–17,21,22,38–70]. With this in mind, the manufactured CFs show the highest mechanical properties publicized so far, see Figure 4.

Furthermore, the present study indicates that a transition of the extensively developed batch-manufactured carbon fibers with even higher lignin contents should be explored for their adaptation and validation in continuous processes. This could enable a consistent increase in lignin content up to over 20 wt.-% for future renewable CFs. Finally, the study

shows a way for the future increase in lignin content in continuously produced CFs and thus a way for the proportional reduction in polyacrylonitrile while maintaining sufficient mechanical properties at a high-temperature carbonization level. It is also expected that commercially available PAN could potentially be partially substituted with small amounts of lignin, similar to what was performed in this study. Further investigation is advised. This should be demonstrated in future studies. Building on this, the climate-damaging impact of PAN in the carbon fiber industry could be gradually reduced.
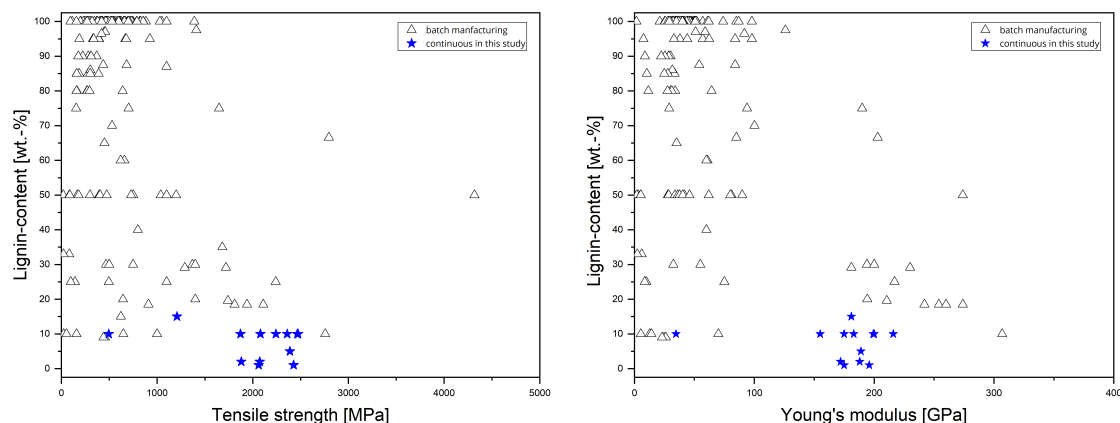
Figure 4. Comparison of the tensile strength (**left**) and Young's modulus (**right**) of blend CFs made from lignin and synthetic polymers produced in batch process by literature and in a continuous process in this study.

Abbreviations

The following abbreviations are used in this manuscript:

AcL	Acetylated lignin
LS	Lignosulfonate
AcLi/LSi	Samples with weight percentage i of AcL resp. LS
CFs	Carbon fibers
DIN	German institute for standards
DMSO	Dimethyl sulfoxide
DMF	Dimethylformamide
DSC	Differential scanning calorimetry
DOAJ	Directory of open access journals
HZi	Heating zone i
MDPI	Multidisciplinary Digital Publishing Institute

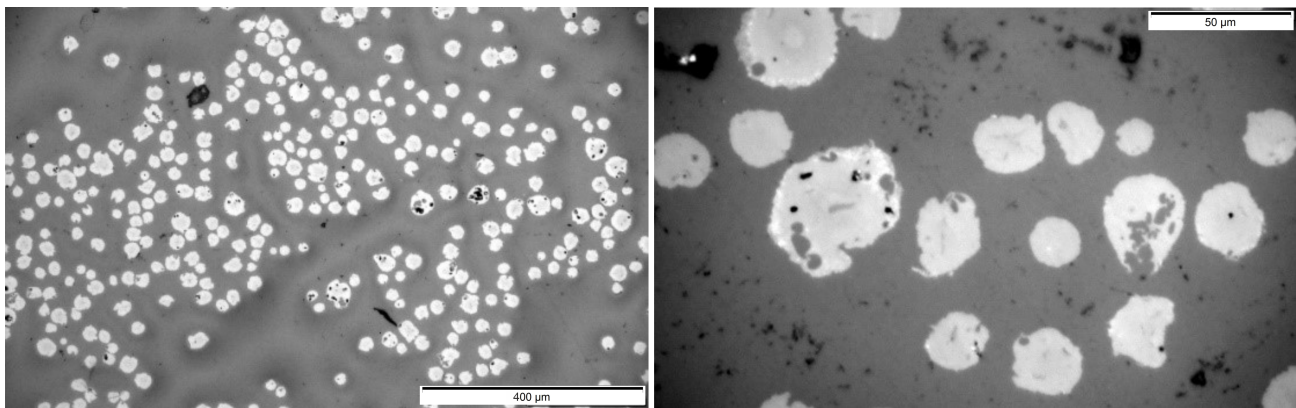| PAN	Polyacrylonitrile
PF	Precursor fiber
SI	Stabilization index
TGA	Thermogravimetrical analysis
DTG	Derivative Thermogravimetry
SD	Standard deviation

Appendix A

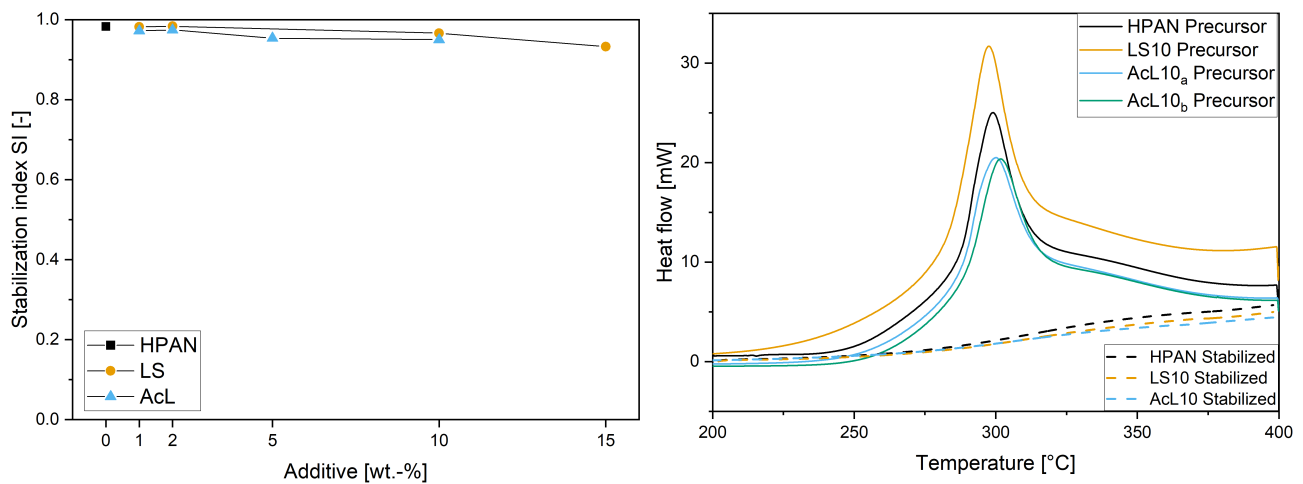**Figure A1.** Cross section area of *LS*20 fiber batch stabilized for 120 min.

Figure A2. Stabilization index (SI) of stabilized fibers with different lignin contents (**left**) and exemplary selected DSC-curves of precursor and stabilized fibers (**right**).

Table A1. Filament diameter (d_F) and mechanical properties—tensile strength (σ), tensile modulus (E), and elongation at break (ε)—of the continuously manufactured Lignin/PAN-blend carbon fibers. The standard deviation (SD) is given for each parameter. The parameter is written in subscript.

| Label	x_{Lig}	Lig	d_F [μm]	SD_{d_F} [μm]	σ [MPa]	SD_{σ} [MPa]	E [GPa]	SD_E [GPa]	ε [%]	SD_{ε} [%]
PAN	-		7.89	0.58	2379	379	207	9	1.19	0.19
*LS*1	1	LS	8.33	0.60	2062	332	175	14	1.25	0.17
*LS*2	2	LS	8.43	0.85	1880	295	188	22	1.04	0.14
*LS*10	10	LS	7.91	0.99	2242	311	216	15	1.09	0.13
*LS*15	15	LS	8.54	1.22	1209	296	181	14	0.69	0.14
*AcL*1	1	AcL	8.16	1.02	2428	271	196	13	1.33	0.13
*AcL*2	2	AcL	8.85	0.89	2073	226	172	12	1.28	0.14
*AcL*5	5	AcL	8.14	1.06	2389	299	189	15	1.34	0.14
*AcL*10a	10	AcL	7.50	1.48	2466	425	200	28	1.31	0.12
*AcL*10b	10	AcL	8.20	1.09	2360	362	183	22	1.36	0.14
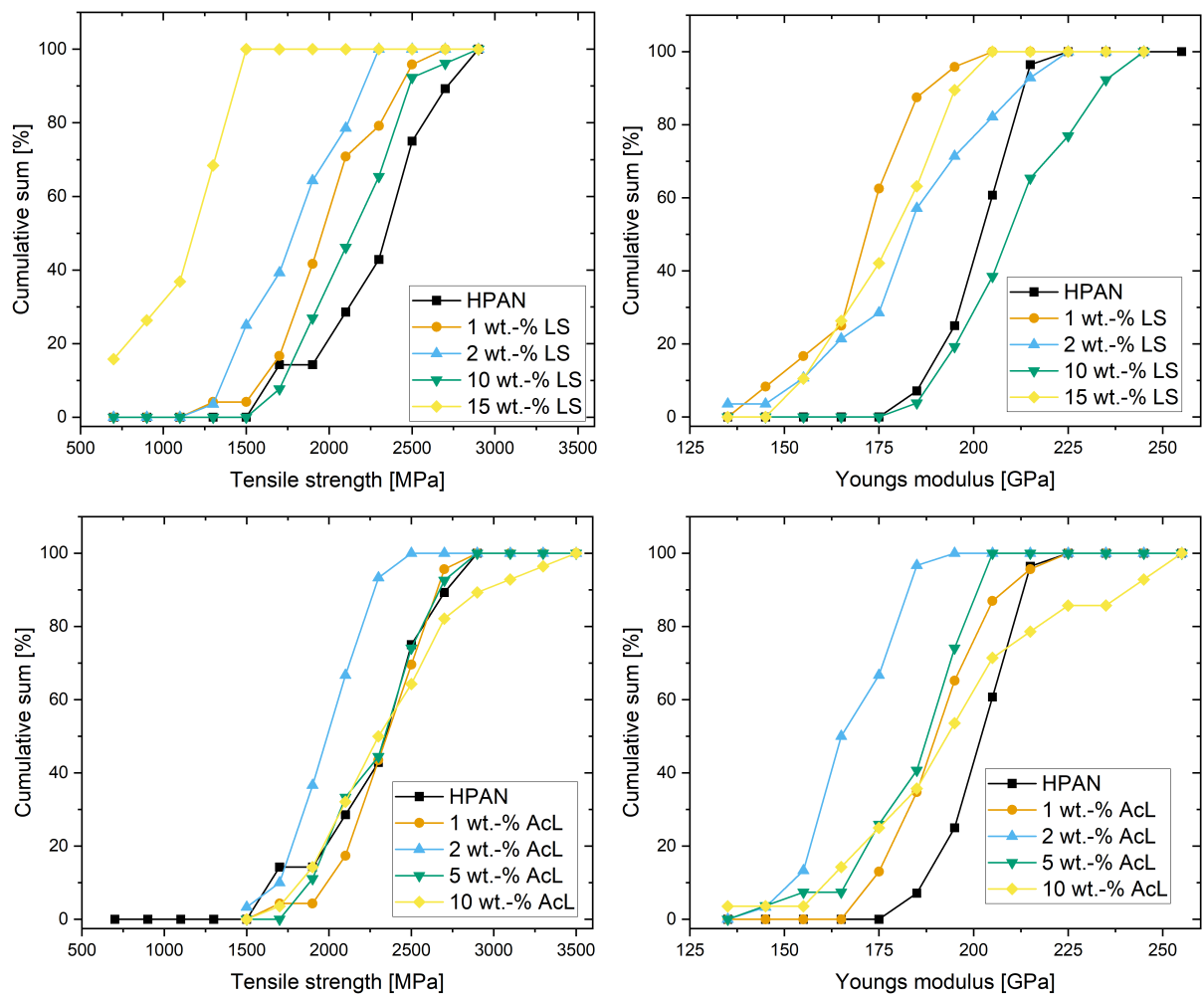
Figure A3. Cumulative distribution graphs of tensile strength (σ) (**left**) and Young's modulus (E) (**right**) for all of the produced fibers (**LS top**; **AcL bottom**).

Table A2. Shape parameters (k) and scale parameters (θ) of gamma distribution fit of the tensile strengths (σ) and Young's moduli (E).

Label	Gamma Distribution of σ		Gamma Distribution Parameters of E	
Parameter	k_σ	θ_σ	k_E	θ_E
PAN	37.4	63.5	561	0.34
*LS*1	37.6	54.8	157	1.12
*LS*2	40.6	46.3	75.8	2.50
*LS*10	53.2	42.1	214	1.00
*LS*15	15.3	79.0	170	1.07
*AcL*1	78.2	31.0	254	0.77
*AcL*2	82.7	25.1	200	0.86
*AcL*5	65.2	36.6	147	1.29
*Acl*10	35.8	68.9	51.5	3.89
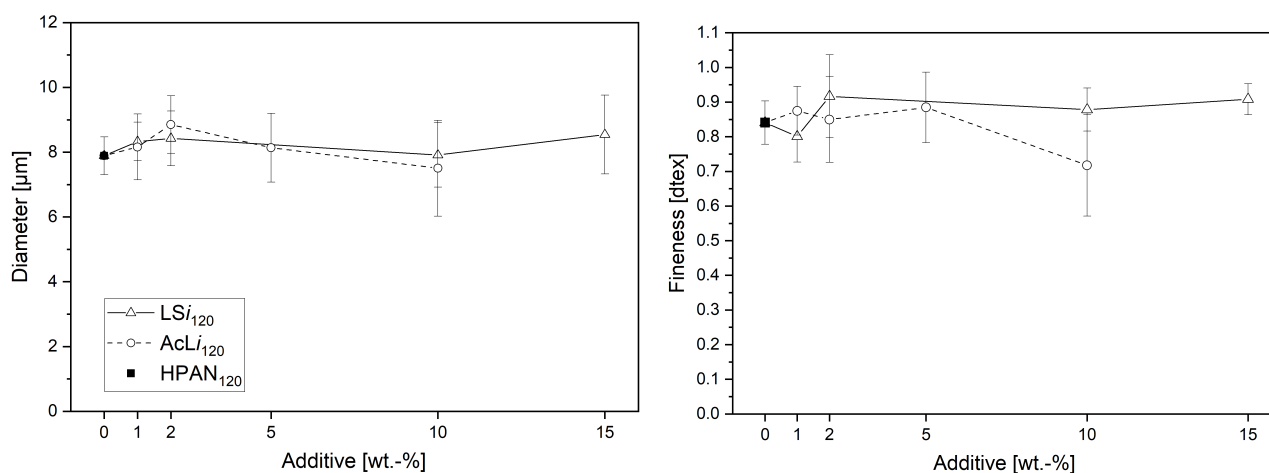
Figure A4. CFs diameter (**left**) and fineness (**right**) for lignosulfonate (LS) and acetylated lignin (AcL)/PAN-blend CFs with different lignin contents.

References

1. Choi, D.; Kil, H.-S.; Lee, S. Fabrication of Low-Cost Carbon Fibers Using Economical Precursors and Advanced Processing Technologies. *Carbon* **2019**, *142*, 610–649. [CrossRef]
2. Jäger, H.; Cherif, C.; Kirsten, M.; Behnisch, T.; Wolz, D.S.; Böhm, R.; Gude, M. Influence of Processing Parameters on the Properties of Carbon Fibers—An Overview. *Mater. Werkst.* **2016**, *47*, 1044–1057. [CrossRef]
3. Böhm, R.; Thieme, M.; Wohlfahrt, D.; Wolz, D.S.; Richter, B.; Jäger, H. Reinforcement Systems for Carbon Concrete Composites Based on Low-Cost Carbon Fibres. *Fibers* **2018**, *6*, 56. [CrossRef]
4. Wang, S.; Bai, J.; Innocent, M.T.; Wang, Q.; Xiang, H.; Tang, J.; Zhu, M. Lignin-Based Carbon Fibers: Formation, Modification and Potential Applications. *Green Energy Environ.* **2022**, *7*, 578–605. [CrossRef]
5. Baker, D.A.; Rials, T.G. Recent Advances in Low-Cost Carbon Fibre Manufacture from Lignin. *J. Appl. Polym. Sci.* **2013**, *130*, 713–728. [CrossRef]
6. Qu, W.; Yang, J.; Sun, X.; Bai, X.; Jin, H.; Zhang, M. Towards Producing High-Quality Lignin-Based Carbon Fibers: A Review of Crucial Factors Affecting Lignin Properties and Conversion Techniques. *Int. J. Biol. Macromol.* **2021**, *189*, 768–784. [CrossRef] [PubMed]
7. Ogale, A.A.; Zhang, M.; Jin, J. Recent advances in carbon fibres derived from biobased precursors. *J. Appl. Polym. Sci.* **2016**, *133*, 43794. [CrossRef]
8. Sagues, W.J.; Jain, A.; Brown, D.; Aggarwal, S.; Suarez, A.; Kollman, M.; Park, S.; Argyropoulos, D.S. Are Lignin-Derived Carbon Fibers Graphitic Enough? *Green Chem.* **2019**, *21*, 4253–4265. [CrossRef]
9. Mack, D.; Berthold, L.-S.; Traa, Y.; Klemm, E. New Two-Step Pathway for the Production of Acrylonitrile from Propionic Acid. *Catal. Commun.* **2020**, *136*, 105891. [CrossRef]
10. Mack, D.; Schätzle, S.; Traa, Y.; Klemm, E. Synthesis of Acrylonitrile from Renewable Lactic Acid. *ChemSusChem* **2019**, *12*, 1653–1663. [CrossRef]
11. Arnold, U.; Brück, T.; De Palmenaer, A.; Kuse, K. Carbon Capture and Sustainable Utilization by Algal Polyacrylonitrile Fiber Production: Process Design, Techno-Economic Analysis, and Climate Related Aspects. *Ind. Eng. Chem. Res.* **2018**, *57*, 7922–7933. [CrossRef]
12. Song, L.; Ouyang, Q.; Huang, X.; Ma, H.; Chen, P.; Shen, L.; Wang, X. Carbon Fibers with Low Cost and Uniform Disordered Structure Derived from Lignin/Polyacrylonitrile Composite Precursors. *Fibers Polym.* **2021**, *22*, 240–248. [CrossRef]
13. Zhang, B.; Lu, C.; Liu, Y.; Yuan, S. Wet Spun Polyacrylonitrile-Based Hollow-Mesoporous Carbon Fiber: Stabilization, Carbonization and Its Basic Properties. *Polym. Degrad. Stab.* **2019**, *170*, 109021. [CrossRef]
14. Liu, H.C.; Luo, J.; Chang, H.; Bakhtiary Davijani, A.A.; Wang, P.-H.; Kumar, S. Polyacrylonitrile Sheath and Polyacrylonitrile/Lignin Core Bi-Component Carbon Fibers. *Carbon* **2019**, *149*, 165–172. [CrossRef]
15. Liu, H.; Dai, Z.; Cao, Q.; Shi, X.; Wang, X.; Li, H.; Han, Y.; Li, Y.; Zhou, J. Lignin/Polyacrylonitrile Carbon Fibers: The Effect of Fractionation and Purification on Properties of Derived Carbon Fibers. *ACS Sustain. Chem. Eng.* **2018**, *6*, 8554–8562. [CrossRef]
16. Liu, D.; Ouyang, Q.; Jiang, X.; Ma, H.; Chen, Y.; He, L. Thermal Properties and Thermal Stabilization of Lignosulfonate-Acrylonitrile-Itaconic Acid Terpolymer for Preparation of Carbon Fiber. *Polym. Degrad. Stab.* **2018**, *150*, 57–66. [CrossRef]
17. Jin, J.; Ogale, A.A. Carbon Fibers Derived from Wet-Spinning of Equi-Component Lignin/Polyacrylonitrile Blends. *J. Appl. Polym. Sci.* **2018**, *135*, 45903. [CrossRef]

18. Jin, J.; Ding, J.; Klett, A.; Thies, M.C.; Ogale, A.A. Carbon Fibers Derived from Fractionated–Solvated Lignin Precursors for Enhanced Mechanical Performance. *ACS Sustain. Chem. Eng.* **2018**, *6*, 14135–14142. [CrossRef]

19. Maradur, S.P.; Kim, C.H.; Kim, S.Y.; Kim, B.-H.; Kim, W.C.; Yang, K.S. Preparation of Carbon Fibers from a Lignin Copolymer with Polyacrylonitrile. *Synth. Met.* **2012**, *162*, 453–459. [CrossRef]

20. Jiang, X.; Ouyang, Q.; Liu, D.; Huang, J.; Ma, H.; Chen, Y.; Wang, X.; Sun, W. Preparation of low-cost carbon fibre precursors from blends of wheat straw lignin and commercial textile-grade polyacrylonitrile (PAN). *Wood Res. Technol.* **2018**, *72*, 727–734. Available online: https://www.degruyter.com/view/j/hfsg.2018.72.issue-9/hf-2017-0191/hf-2017-0191.xml (accessed on 5 March 2023).

21. Liu, H.C.; Chien, A.-T.; Newcomb, B.A.; Liu, Y.; Kumar, S. Processing, Structure, and Properties of Lignin- and CNT-Incorporated Polyacrylonitrile-Based Carbon Fibers. *ACS Sustain. Chem. Eng.* **2015**, *3*, 1943–1954. [CrossRef]

22. Xia, K.; Ouyang, Q.; Chen, Y.; Wang, X.; Qian, X.; Wang, L. Preparation and Characterization of Lignosulfonate–Acrylonitrile Copolymer as a Novel Carbon Fiber Precursor. *ACS Sustain. Chem. Eng.* **2016**, *4*, 159–168. [CrossRef]

23. Dér, A.; Dilger, N.; Kaluza, A.; Creighton, C.; Kara, S.; Varley, R.; Herrmann, C.; Thiede, S. Modelling and Analysis of the Energy Intensity in Polyacrylonitrile (PAN) Precursor and Carbon Fibre Manufacturing. *J. Clean. Prod.* **2021**, *303*, 127105. [CrossRef]

24. Groetsch, T.; Maghe, M.; Rana, R.; Hess, R.; Nunna, S.; Herron, J.; Buckmaster, D.; Creighton, C.; Varley, R.J. Gas Emission Study of the Polyacrylonitrile-Based Continuous Pilot-Scale Carbon Fiber Manufacturing Process. *Ind. Eng. Chem. Res.* **2021**, *60*, 17379–17389. [CrossRef]

25. Groetsch, T.; Creighton, C.; Varley, R.; Kaluza, A.; Dér, A.; Cerdas, F.; Herrmann, C. A Modular LCA/LCC-Modelling Concept for Evaluating Material and Process Innovations in Carbon Fibre Manufacturing. *Procedia CIRP* **2021**, *98*, 529–534. [CrossRef]

26. Dong, X.; Lu, C.; Zhou, P.; Zhang, S.; Wang, L.; Li, D. Polyacrylonitrile/lignin sulfonate blend fibre for low-cost carbon fibre. *RSC Adv.* **2015**, *5*, 42259–42265. Available online: https://pubs.rsc.org/en/content/articlelanding/2015/ra/c5ra01241d#!divAbstract (accessed on 13 August 2023). [CrossRef]

27. Porkodi, P.; Abhilash, J.K.; Shukla, H.K. On the Structural Changes, Mechanism and Kinetics of Stabilization of Lignin Blended Polyacrylonitrile Copolymer Fiber. *J. Polym. Res.* **2022**, *29*, 436. [CrossRef]

28. Kirsten, M.; Meinl, J.; Schönfeld, K.; Michaelis, A.; Cherif, C. Characteristics of wet-spun and thermally treated poly acrylo-nitrile fibres. *J. Appl. Polym. Sci.* **2016**, *133*, 43698. [CrossRef]

29. Gohs, U.; Böhm, R.; Brünig, H.; Fischer, D.; Häussler, L.; Kirsten, M.; Malanin, M.; Müller, M.-T.; Cherif, C.; Wolz, D.S.J.; et al. Electron beam treatment of polyacrylonitrile copolymer above the glass transition temperature in air and nitrogen at-mosphere. *Radiat. Phys. Chem.* **2019**, *156*, 22–30. [CrossRef]

30. Gohs, U.; Böhm, R.; Brünig, H.; Fischer, D.; Leopold, A.-K.; Malanin, M.; Müller, M.-T.; Cherif, C.; Richter, M.; Wolz, D.S.J.; et al. Influence of gas atmosphere on electron-induced reactions of polyacrylonitrile homopolymer powder at elevated temperature. *Radiat. Phys. Chem.* **2019**, *158*, 94–102. [CrossRef]

31. Kirsten, M.; Freudenberg, C.; Cherif, C. Carbonfasern—Der Werkstoff des 21. Jahrhunderts. *Beton- Stahlbetonbau* **2015**, *110*, 8–15. [CrossRef]

32. Sadeghi Bogar, M.; Wolf, J.; Wolz, D.S.J.; Seidel-Greiff, R.; Dmitrieva, E.; Israel, N.; Rosenkranz, M.; Behnisch, T.; Müller, M.T.; Gude, M. Sensitivity of Offline and Inline Indicators for Fiber Stretching in Continuous Polyacrylonitrile Stabilization. *Fibers* **2023**, *11*, 68. [CrossRef]

33. Byrne, N.; De Silva, R.; Ma, Y.; Sixta, H.; Hummel, M. Enhanced stabilization of cellulose-lignin hybrid filaments for carbon fiber production. *Cellulose* **2018**, *25*, 723–733. [CrossRef] [PubMed]

34. *DIN 65569-2:1992-10*; Aerospace; Reinforcement Fibres; Determination of Density of Filament Yarns; Hydrostatic Weighing Method. German Institute for Standardisation: Berlin, Germany, 1992. Available online: https://www.beuth.de/de/norm/din-65569-2/1944125 (accessed on 5 May 2023).

35. Tsai, J.-S.; Hsu, H.-N. Determination of the Aromatization Index for Oxidized Polyacrylonitrile Fibre by the Differential Scanning Calorimetry Method. *J. Mater. Sci. Lett.* **1992**, *11*, 1403–1405. [CrossRef]

36. Takaku, A.; Hashimoto, T.; Miyoshi, T. Tensile Properties of Carbon Fibers from Acrylic Fibers Stabilized under Isothermal Conditions. *J. Appl. Polym. Sci.* **1985**, *30*, 1565–1571. [CrossRef]

37. Fitzer, E.; Frohs, W.; Heine, M. Optimization of Stabilization and Carbonization Treatment of PAN Fibres and Structural Characterization of the Resulting Carbon Fibres. *Carbon* **1986**, *24*, 387–395. [CrossRef]

38. Ding, R.; Wu, H.; Thunga, M.; Bowler, N.; Kessler, M.R. Processing and Characterization of Low-Cost Electrospun Carbon Fibers from Organosolv Lignin/Polyacrylonitrile Blends. *Carbon* **2016**, *100*, 126–136. [CrossRef]

39. Attwenger, A. Value-Added Lignin Based Carbon Fiber from Organosolv Fractionation of Poplar and Switchgrass. Master's Thesis, University of Tennessee, Knoxville, TN, USA, 2014. Available online: http://trace.tennessee.edu/utk_gradthes/2768 (accessed on 7 December 2022).

40. Baker, D.A.; Baker, F.S.; Gallego, N.C. Thermal Engineering of Lignin for Low-Cost Production of Carbon Fiber. In Proceedings of the The Fiber Society 2009 Fall Meeting and Technical Conference, Athens, GA, USA, 28–30 October 2009.

41. Baker, D.A.; Gallego, N.C.; Baker, F.S. On the Characterization and Spinning of an Organic-Purified Lignin toward the Manufacture of Low-Cost Carbon Fiber. *J. Appl. Polym. Sci.* **2012**, *124*, 227–234. [CrossRef]

42. Eberle, C. R&D on Low—Cost Carbon Fiber Composites for Energy Applications. *Carbon Fiber RD Workshop* **2013**, *25*.
43. Hosseinaei, O.; Harper, D.P.; Bozell, J.J.; Rials, T.G. Improving Processing and Performance of Pure Lignin Carbon Fibers through Hardwood and Herbaceous Lignin Blends. *Int. J. Mol. Sci.* **2017**, *18*, 1410. [CrossRef]
44. Hosseinaei, O.; Harper, D.P.; Bozell, J.J.; Rials, T.G. Role of Physicochemical Structure of Organosolv Hardwood and Herbaceous Lignins on Carbon Fiber Performance. *ACS Sustain. Chem. Eng.* **2016**. [CrossRef]
45. Kadla, J.F.; Kubo, S.; Venditti, R.A.; Gilbert, R.D.; Compere, A.L.; Griffith, W. Lignin-Based Carbon Fibers for Composite Fiber Applications. *Carbon* **2002**, *40*, 2913–2920. [CrossRef]
46. Kleinhans, J. Evaluation of the Carbonization of Thermo-Stabilized Lignin Fibers into Carbon Fibers. Master's Thesis, Universität Linköping, Linköping, Sweden, 2015. Available online: http://www.diva-portal.org/smash/get/diva2:846024/FULLTEXT01.pdf (accessed on 28 September 2016).
47. Kubo, S.; Kadla, J.F. Lignin-Based Carbon Fibers: Effect of Synthetic Polymer Blending on Fiber Properties. *J. Polym. Environ.* **2005**, *13*, 97–105. [CrossRef]
48. Nordström, Y.; Joffe, R.; Sjöholm, E. Mechanical Characterization and Application of Weibull Statistics to the Strength of Softwood Lignin-Based Carbon Fibers. *J. Appl. Polym. Sci.* **2013**, *130*, 3689–3697. [CrossRef]
49. Qin, W.; Kadla, J.F. Carbon Fibers Based on Pyrolytic Lignin. *J. Appl. Polym. Sci.* **2012**, *126*, E204–E213.2. [CrossRef]
50. Qu, W.; Xue, Y.; Gao, Y.; Rover, M.; Bai, X. Repolymerization of Pyrolytic Lignin for Producing Carbon Fiber with Improved Properties. *Biomass Bioenergy* **2016**, *95*, 19–26. [CrossRef]
51. Qu, W.; Liu, J.; Xue, Y.; Wang, X.; Bai, X. Potential of Producing Carbon Fiber from Biorefinery Corn Stover Lignin with High Ash Content. *J. Appl. Polym. Sci.* **2018**, *135*, 45736. [CrossRef]
52. Salmén, L.; Bergnor, E.; Olsson, A.-M.; Åkerström, M.; Uhlin, A. Extrusion of Softwood Kraft Lignins as Precursors for Carbon Fibres. *BioResources* **2015**, *10*, 7544–7554. [CrossRef]
53. Sudo, K.; Shimizu, K. A New Carbon Fiber from Lignin. *J. Appl. Polym. Sci.* **1992**, *44*, 127–134. [CrossRef]
54. Uraki, Y.; Kubo, S.; Nigo, N.; Sano, Y.; Sasaya, T. Preparation of Carbon Fibers from Organosolv Lignin Obtained by Aqueous Acetic Acid Pulping. *Holzforsch. Int. J. Biol. Chem. Phys. Technol. Wood* **1995**, *49*, 343–350. [CrossRef]
55. Zhang, M.; Ogale, A.A. Carbon Fibers from Dry-Spinning of Acetylated Softwood Kraft Lignin. *Carbon* **2014**, *69*, 626–629. [CrossRef]
56. Zhang, M.; Jin, J.; Ogale, A.A. Carbon Fibers from UV-Assisted Stabilization of Lignin-Based Precursors. *Fibers* **2015**, *3*, 184–196. [CrossRef]
57. Zhang, M. Carbon Fibers Derived from Dry-Spinning of Modified Lignin Precursors. Ph.D. Thesis, Clemson University, Clemson, SC, USA, 2016. Available online: http://tigerprints.clemson.edu/all_dissertations/1616 (accessed on 8 May 2023).
58. Wang, S.; Li, Y.; Xiang, H.; Zhou, Z.; Chang, T.; Zhu, M. Low Cost Carbon Fibers from Bio-Renewable Lignin/Poly(Lactic Acid) (PLA) Blends. *Compos. Sci. Technol.* **2015**, *119*, 20–25. [CrossRef]
59. Kanhere, S.V.; Tindall, G.W.; Ogale, A.A.; Thies, M.C. Carbon Fibers Derived from Liquefied and Fractionated Poplar Lignins: The Effect of Molecular Weight. *iScience* **2022**, *25*, 105449. [CrossRef] [PubMed]
60. Bostan, L.; Hosseinaei, O.; Fourn, R.; Herrmann, A.S. Upscaling of Lignin Precursor Melt Spinning by Bicomponent Spinning and Its Use for Carbon Fibre Production. *Philos. Trans. R. Soc.* **2021**, *379*, 2209. [CrossRef]
61. Culebras, M.; Beaucamp, A.; Wang, Y.; Clauss, M.M.; Frank, E.; Collins, M.N. Biobased Structurally Compatible Polymer Blends Based on Lignin and Thermoplastic Elastomer Polyurethane as Carbon Fiber Precursors. *ACS Sustain. Chem. Eng.* **2018**, *6*, 8816–8825. [CrossRef]
62. Geng, L.; Cai, Y.; Lu, L.; Zhang, Y.; Li, Y.; Chen, B.; Peng, X.-F. Highly Strong and Conductive Carbon Fibers Originated from Bioinspired Lignin/Nanocellulose Precursors Obtained by Flow-Assisted Alignment and In Situ Interfacial Complexation. *ACS Sustain. Chem. Eng.* **2021**, *9*, 2591–2599. [CrossRef]
63. Lin, J.; Kubo, S.; Yamada, T.; Koda, K.; Uraki, Y. Chemical Thermostabilization for the Preparation of Carbon Fibers from Softwood Lignin. *BioResources* **2012**, *7*, 5634–5646. [CrossRef]
64. Li, Q.; Hu, C.; Li, M.; Truong, P.; Li, J.; Lin, H.-S.; Naik, M.T.; Xiang, S.; Jackson, B.E.; Kuo, W.; et al. Enhancing the Multi-Functional Properties of Renewable Lignin Carbon Fibers via Defining the Structure–Property Relationship Using Different Biomass Feedstocks. *Green Chem.* **2021**, *23*, 3725–3739. [CrossRef]
65. Dai, Z.; Shi, X.; Liu, H.; Li, H.; Han, Y.; Zhou, J. High-Strength Lignin-Based Carbon Fibers via a Low-Energy Method. *RSC Adv.* **2018**, *8*, 1218–1224. [CrossRef]
66. Zhang, W.; Wang, M.; Liu, W.; Yang, C.; Wu, G. Higher Dose Rate Effect of 500-KeV EB Irradiation Favoring Free Radical Annealing and Pre-Oxidation of Polyacrylonitrile Fibers. *Polym. Degrad. Stab.* **2019**, *167*, 201–209. [CrossRef]
67. Ouyang, Q.; Xia, K.; Liu, D.; Jiang, X.; Ma, H.; Chen, Y. Fabrication of Partially Biobased Carbon Fibers from Novel Lignosulfonate–Acrylonitrile Copolymers. *J. Mater. Sci.* **2017**, *52*, 7439–7451. [CrossRef]
68. Qu, W.; Bai, X. Thermal Treatment of Pyrolytic Lignin and Polyethylene Terephthalate toward Carbon Fiber Production. *J. Appl. Polym. Sci.* **2020**, *137*, 48843. [CrossRef]

69. Enengl, C.; Lumetzberger, A.; Duchoslav, J.; Mardare, C.C.; Ploszczanski, L.; Rennhofer, H.; Unterweger, C.; Stifter, D.; Fürst, C. Influence of the Carbonization Temperature on the Properties of Carbon Fibers Based on Technical Softwood Kraft Lignin Blends. *Carbon Trends* **2021**, *5*, 100094. [CrossRef]

70. Kim, M.S.; Lee, D.H.; Kim, C.H.; Lee, Y.J.; Hwang, J.Y.; Yang, C.-M.; Kim, Y.A.; Yang, K.S. Shell–Core Structured Carbon Fibers via Melt Spinning of Petroleum- and Wood-Processing Waste Blends. *Carbon* **2015**, *85*, 194–200. [CrossRef]